Journal of ELECTRONIC MATERIALS, Vol. 38, No. 2, 2009
DOI: 10.1007/s11664-008-0562-9
© 2008 TMS
Special Issue Paper

Temperature-Dependent Phase Segregation in Cu/42Sn-58Bi/Cu Reaction Couples under High Current Density

GUANGCHEN XU,[1] HONGWEN HE,[1] and FU GUO[1,2]

1.—College of Materials Science and Engineering, Beijing University of Technology, Beijing, China. 2.—e-mail: guofu@bjut.edu.cn

The effects of current stressing at 10^4 A/cm^2 on Cu/42Sn-58Bi/Cu reaction couples with a one-dimensional structure at 23°C, 50°C, and 114°C were investigated. The microstructural evolution during electromigration was examined using scanning electron microscopy. The temperature dependence of the coarsening of the Bi-rich phase, the dominant migrating entity, and hillock/whisker formation in eutectic Sn-Bi were investigated under high current density. During current stressing at 10^4 A/cm^2, the average size of the Bi-rich phase remained the same at 23°C, increased at 50°C, and shrank at 140°C. Bi accumulated near the anode side at both high (50°C, 140°C) and low temperature (23°C). At high temperatures, both Sn and Bi diffused towards the anode side, but Bi moved ahead of Sn during current stressing. However, at low temperatures, Sn reversed its direction of migration to the cathode side. Pure Bi hillocks/whiskers and a mixed structure of Sn and Bi hillocks were extruded as a consequence of compressive stress from electromigration-induced mass flow towards the anode side.

Key words: Electromigration, Joule heating, eutectic Sn-Bi

INTRODUCTION

Mass movement resulting from the imposition of high current density is known as electromigration (EM). The basic issues involving the movement of conductive constituents and microstructural evolution due to high current density in single-phase materials are well documented.[1,2] Unlike EM behavior in single-phase materials, electronic solders used in interconnects are multiphase materials designed to accommodate various manufacturing and service-related issues.[3,4] Below its eutectic temperature, the microstructure of a eutectic alloy consists of two primary phases according to its eutectic phase diagram. It is possible to have near-complete phase separation into two parts under an external driving force. Indeed, this has been shown to occur in EM in eutectic Sn-Pb solder joints at 150°C by Brandenburg and Yeh, where the Pb moved and accumulated towards the anode side, and the Sn towards the cathode side.[5] However, it was also reported, in the same eutectic Sn-Pb alloy, that Sn and Pb reversed their diffusion direction when EM was conducted at room temperature.[6–8]

It is generally accepted that temperature is a key factor influencing the diffusion mechanism of EM in eutectic binary solder alloys. The industry is currently moving towards Pb-free solder materials due to health and environmental concerns. Due to its lower melting point and lower coefficient of thermal expansion compared with eutectic Sn-Pb alloy, eutectic Sn-Bi alloy is a Pb-free solder with great potential in applications that are sensitive to temperature or thermal damage.[9] However, low-melting-point solders are sensitive to high current density. Recent work on the EM behavior of eutectic Sn-Bi solder joints showed that Bi segregated towards the interface at the anode side at high temperatures (>70°C),[9–12] but few researchers have provided systematic discussions of EM diffusion mechanisms in eutectic solder materials at both low and high temperatures in one study.

(Received April 14, 2008; accepted September 4, 2008; published online October 7, 2008)

To understand the fundamentals of complex interactions, and to investigate failure mechanisms in solder joints at various operating conditions, there is a need to develop an appropriate joint configuration for comparing the reliability of different solder alloys and/or to develop mitigation strategies to combat the deleterious effects of EM. The currently popular joint configuration employed by electronics manufacturers utilizes a circuit with solder bumps. In such a configuration induced current crowding exists due to an extreme thin-thick divergence where local current densities can vary by two or more orders of magnitude over a very short distance.[13] This paper deals with the design of solder reaction couples that can be used to carry out the fundamentally critical studies on the effects of EM as a function of temperature in eutectic Sn-Bi solder in a laboratory environment.

EXPERIMENTAL PROCEDURE

Figure 1a–d shows schematic drawings of the soldering setup for the solder reaction couples. The solder reaction couples with a Cu/42Sn-58Bi/Cu sandwich structure were fabricated to conduct EM studies as shown in Fig. 1a. Two copper wires (diameter 500 μm) were first placed into a soldering die with U-grooves, one of which was connected to an *X-Y-Z* adjusting system so that the Cu wires could be well aligned with a controlled gap. The solder thickness can be precisely controlled by using spiral micrometers in such an *X-Y-Z* adjusting system. Then, a 500-μm solder ball with 42Sn-58Bi composition and compatible no-clean flux were both placed into the gap between the two copper wires. Finally, the die with the specimen was heated to 179°C (40°C higher than the melting point of 42Sn-58Pb) and then rapidly cooled to room temperature by using a ventilating fan.

After solder reaction couples were fabricated, they were cold mounted in epoxy resin. In order to achieve a high current density (10^4 A/cm^2), half of the specimen was ground and polished off to reach a cross-sectional area of 1×10^{-3} cm^2. As illustrated in Fig. 1b, two plate-fin coolers were fixed onto the surface of the copper wire cross-section to avoid the over-Joule-heating effect in the solder reaction couples. A current of 10 A was continuously applied to the specimen, corresponding to a current density of 10^4 A/cm^2. Figure 1c shows schematically the specimen under current stressing, and Fig. 1d shows a top view of the solder reaction couples. Three types of testing conditions were designed based on the need to study the effects of current density and ambient temperature. In type I, the specimen was placed at room temperature of 23 ± 1°C. In type II, the specimen was placed in an oven chamber where the temperature was set to 90°C. In type III, the specimen was also placed at room temperature, but equipped with a highly effective heat dissipation fan.

The increased surface temperature of the specimen in types I, II, and III was monitored by using a temperature recorder with K-type thermocouples. As shown in Table I, the increased surface temperature of the specimen in type I was mainly from Joule heating; the increased surface temperature of the specimen in type II was the combined effect of Joule heating and thermal conduction from the oven; and the surface temperature of the specimen in type III was maintained at room temperature because the increased surface temperature induced by Joule heating was dissipated.

Scanning electron microscopy (SEM) was used to observe the microstructural evolution of the solder reaction couples. An energy-dispersive x-ray spectrum was used to help analyze the composition of the detected regions.

RESULTS AND DISCUSSION

Coarsening of the Bi-Rich Phase

The Joule heating effect could not be neglected with a large electrical current (10 A) applied. The surface temperature of the type I cross-section was monitored during the test. As shown in Fig. 2, the temperature rose rapidly initially and approached about 50°C after 30 min.

A square area of 30 μm × 30 μm was randomly selected in the center of the type I cross-section before and after EM. Figure 3 shows SEM images of the microstructural evolution of the eutectic Sn-Bi solder in type I, clearly showing the phenomenon of two-phase separation and Joule-heating-induced coarsening with time and temperature. Figure 3a shows the eutectic Sn-Bi microstructure immediately after solidification. Note the regions of different shades of gray and white, which represent regions of high Sn and high Bi concentration, respectively.

Originally Sn and Bi were dispersed finely; however, this fine mix was eventually superseded by growing islands of high Sn and Bi concentrations after 24 h of current stressing, as shown in Fig. 3c. By using ImageJ™, a public-domain Java-based professional image processing software, quantification of the coarsened Bi-rich phase becomes possible. Before counting and measuring objects in the eutectic Sn-Bi microstructure, the particle analyzer should be configured. By entering a single value of 0.05 μm^2, particles smaller than this value can be ignored. Accordingly, the profiles of the Bi-rich phase before and after EM were obtained by ImageJ™, as shown in Fig. 3b and d, respectively. Under such conditions, the average size of the Bi-rich phase was calculated to be 3.859 μm^2 without current stressing and 5.756 μm^2 after 24 h of current stressing.

Figure 4 shows SEM images of the microstructural evolution of the eutectic Sn-Bi solder in type II. Figure 4a and c illustrates the as-reflowed microstructure and the microstructure after 24 h of current stressing, respectively. The average size of

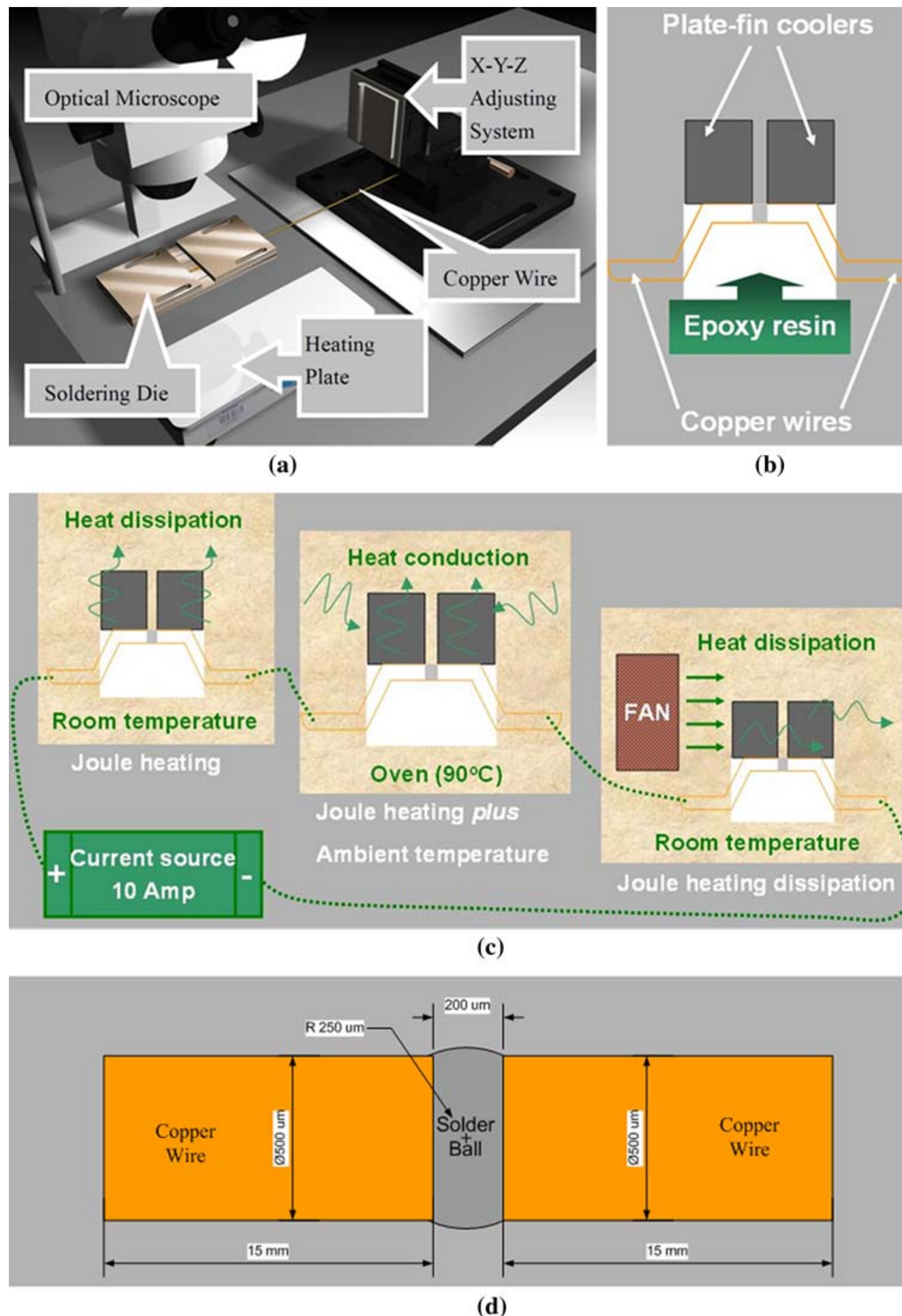

Fig. 1. Schematic diagrams of specimen preparation: (a) soldering setup for the solder reaction couples; (b) solder reaction couples equipped with the plate-fin coolers; (c) solder reaction couples under current stressing; (d) top view of the solder reaction couples.

Table I. Three Types of Testing Conditions, Classified by the Source of Increased Surface Temperature

Type	Source of Increased Surface Temperature
I	Joule heating
II	Joule heating and oven
III	Joule heating dissipation

the Bi-rich phase was calculated to be 7.342 μm^2 before current stressing (Fig. 4b) and 3.363 μm^2 after 24 h of current stressing (Fig. 4d). These fine grains suggested that the solder alloy in type II had melted and solidified. As mentioned above, Joule heating increased the surface temperature of the specimen cross-section from 23°C to 50°C. In addition, the oven temperature in type II was set to 90°C. Thus, the total surface temperature of the

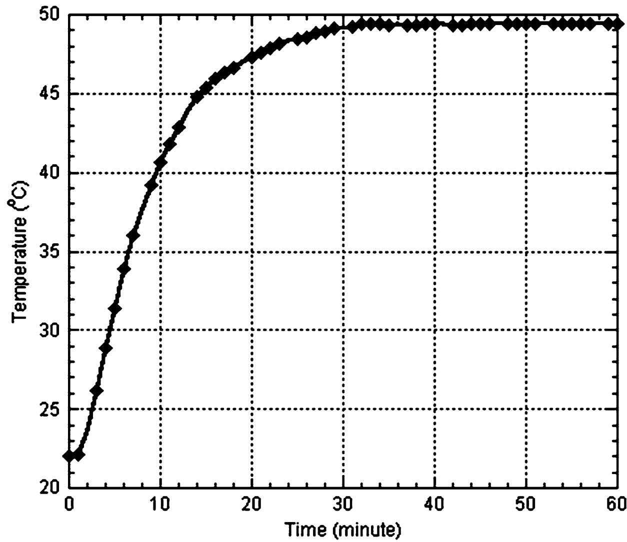

Fig. 2. Temperature profile of the Joule heating effect in type I.

specimen in type II was 140°C, while the melting point of eutectic Sn-Bi is only 138°C. In other words, the specimen in type II was close to molten during the EM test. When the current source was switched off, the type II specimen was removed from the oven for SEM observation, cooling the type II specimen below its melting point. However, thermal input, as illustrated in Fig. 5 presented to characterize the combined effects of the reflow temperature and the time above the liquidus during soldering, was different for the two reflow times. Tao et al.[14] proved that thermal input has a dominant influence on IMC layer formation during soldering. Lee et al.[15] proposed that the IMC morphological microstructure varied depending on the amount of thermal input and the heating rates used in the reflow profile. It could therefore be inferred that the different thermal input in the two melting-solidification processes was the main reason contributing to the decreasing average size of the Bi-rich phase.

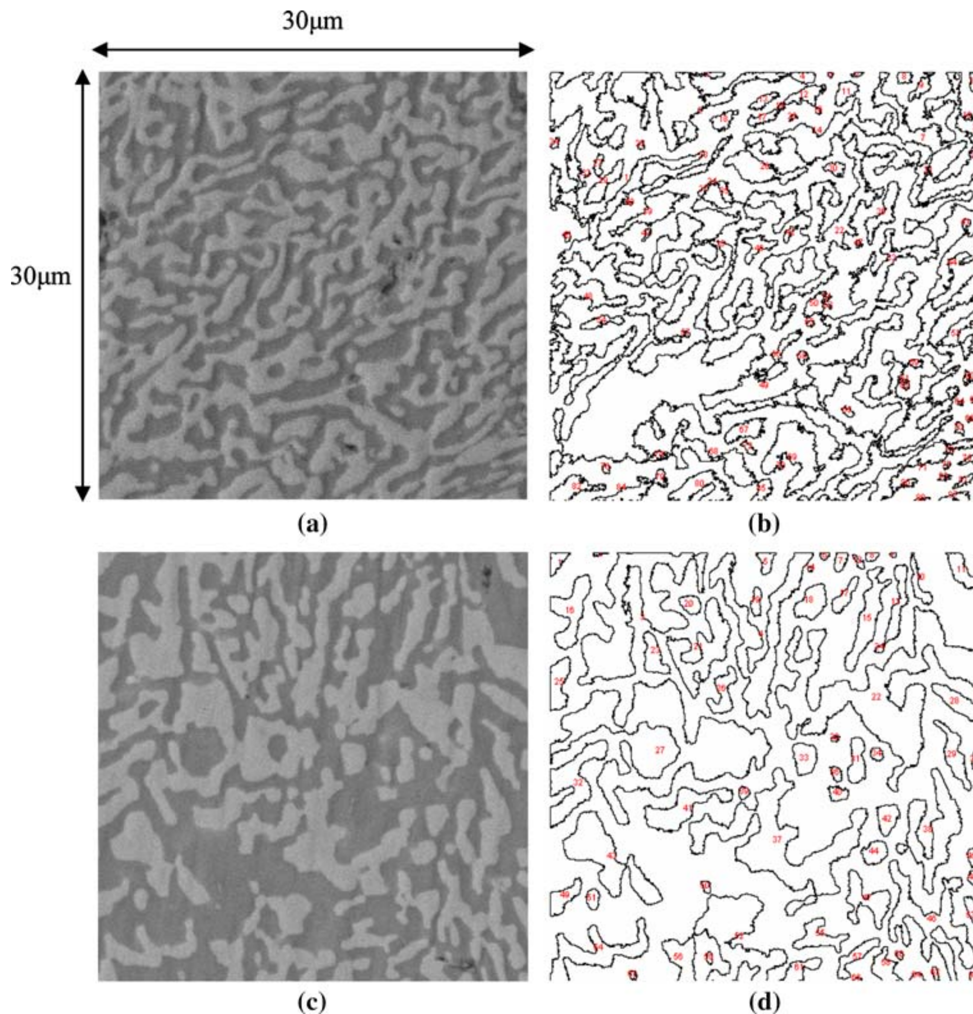

Fig. 3. Microstructural evolution of the eutectic Sn-Bi solder, and the corresponding area calculation of the Bi-rich phase in type I: (a) without current stressing; (b) the profile of the Bi-rich phase in (a) obtained by ImageJ^{TM}; (c) after current stressing for 24 h; (d) the profile of the Bi-rich phase in (c) obtained by ImageJ^{TM}.

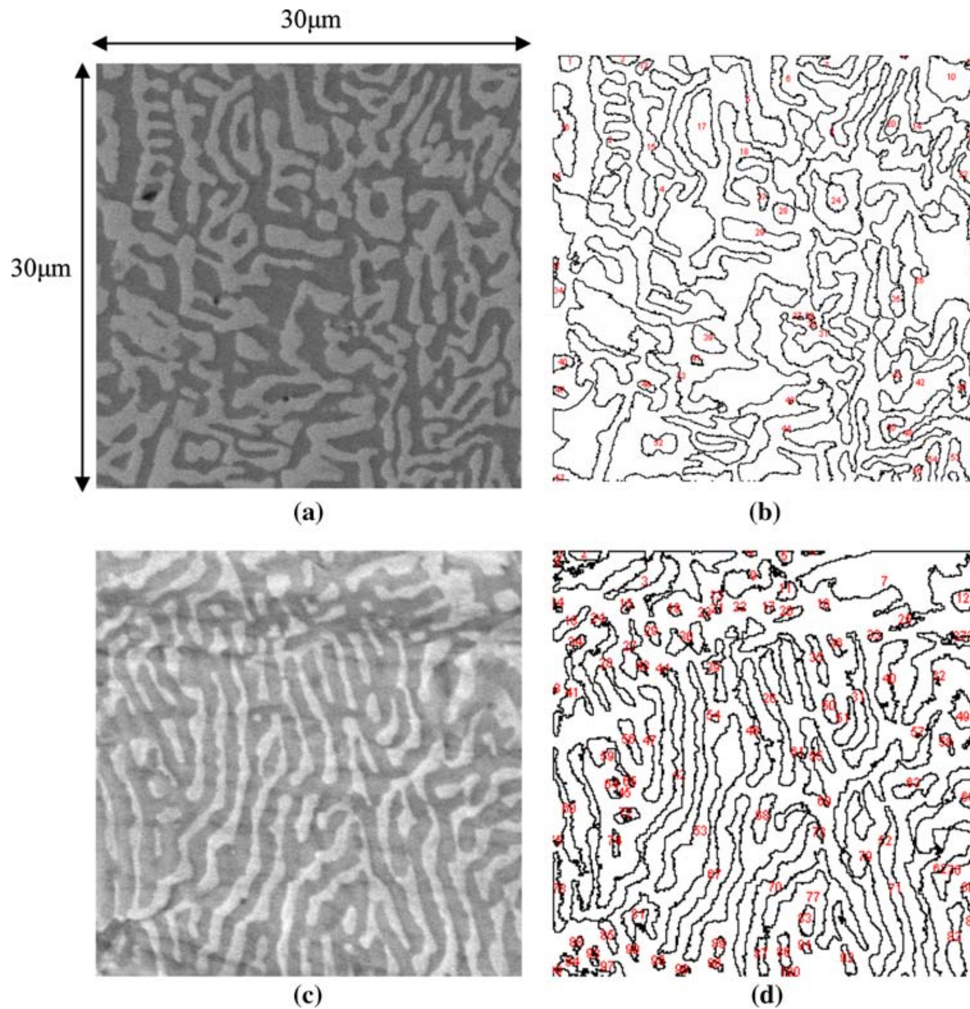

Fig. 4. Microstructural evolution of the eutectic Sn-Bi solder, and the corresponding area calculation of the Bi-rich phase in type II: (a) without current stressing; (b) the profile of the Bi-rich phase in (a) obtained by ImageJ^{TM}; (c) after current stressing for 24 h; (d) the profile of the Bi-rich phase in (c) obtained by ImageJ^{TM}.

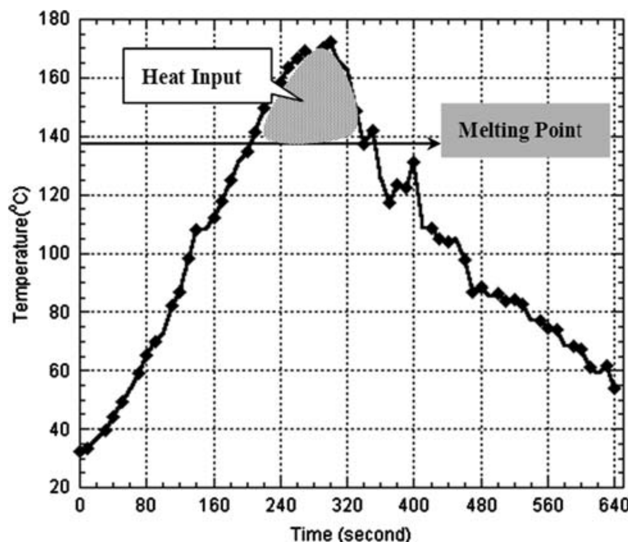

Fig. 5. Temperature profile of the thermal input during the soldering process.

Figure 6a and c shows SEM images of the microstructural evolution of the eutectic Sn-Bi solder in type III. By employing effective Joule heating dissipation devices in the test, the surface temperature of the specimen in type III was maintained approximately at room temperature (23°C) with the high current density. The coarsening tendencies of the Bi-rich phase, as exhibited by type I and II specimens, was not evident in type III. The average size of the Bi-rich phase without current stressing was 4.729 μm^2 (Fig. 6b), but after 24 h of current stressing the size of the Bi-rich phase remains at 4.693 μm^2 (Fig. 6d). The coarsening of the Bi-rich phase was therefore sensitive to the ambient temperature. At a relatively low temperature the size of the Bi-rich phase did not change unless an extremely long storage time was reached.

Phase Accumulation

After the application of a direct current (DC) at a density of 10^4 A/cm^2 for an extended period, the

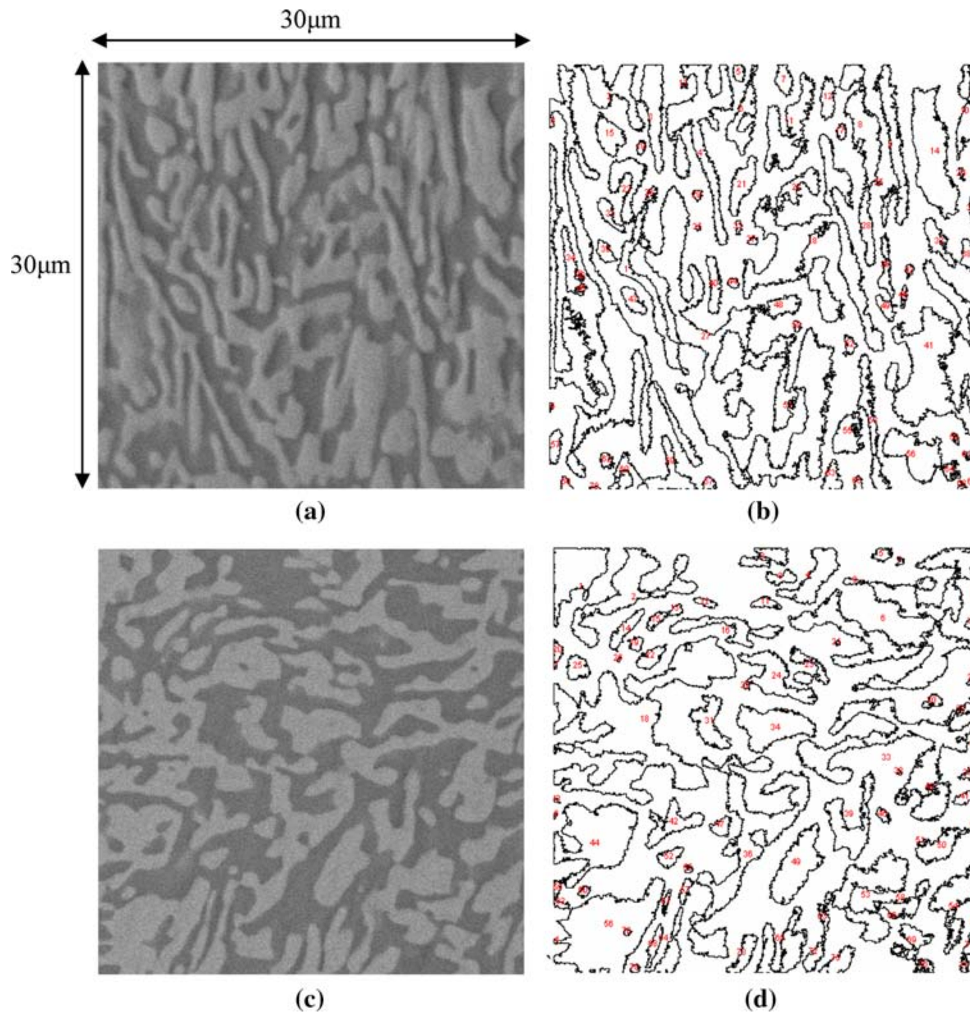

Fig. 6. Microstructural evolution of eutectic Sn-Bi solder, and the corresponding area calculation of the Bi-rich phase in type III: (a) without current stressing; (b) the profile of the Bi-rich phase in (a) obtained by ImageJ^{TM}; (c) after current stressing for 24 h; (d) the profile of the Bi-rich phase in (c) obtained by ImageJ^{TM}.

microstructure in types I and III shared a common characteristic: that the Bi-rich phase accumulated near the anode side whereas the Sn-rich phase accumulated near the cathode side. Due to the remelting process of the specimen in type II, distinct phase accumulation in the solder joint was not observed, so type II is not discussed in this section.

Figure 7a and b shows the interfacial microstructure on the anode side and cathode side after type I was stressed at a current density of 10^4 A/cm^2 for 24 h. As illustrated in Fig. 7a, a layer of Bi-rich phase accumulated at the anode interface, with a mean thickness of about 4 μm. Although the Bi-rich phase was also found at the interface before current stressing, it was broken into isolated networks by the Sn-rich phase. In contrast, the Bi layer formed after current stressing was continuous along the anode interface. As illustrated in Fig. 7b, voids initiated and started to propagate along the cathode interface between the solder matrix and the copper substrate.

Prolonging the current stressing for an additional 100 h caused the eutectic microstructural features to coarsen further, and to elongate in the direction parallel to the electron flow. In this joint total segregation into a two-layer morphology occurred after 133 h as illustrated in Fig. 8a. Figure 8b and c shows the EDX elemental mapping, indicating that the two layers are Bi and Sn, respectively.

In Fig. 9, the growth behavior of the Bi layer in type III was shown to be different from that in type I. In type I, the Bi layer grew rapidly with time. However, in type III, the Bi layer grew at an extremely low rate. After 199 h of current stressing, a layer of Bi accumulated near the anode interface, whereas a layer of Sn accumulated near the cathode interface, as illustrated in Fig. 9a and b. It is interesting to note that no voids initiated and propagated at the cathode interface during the EM test in type III.

Ho et al.[16] presented the movement of both Sn and Pb during the early stages of current stressing

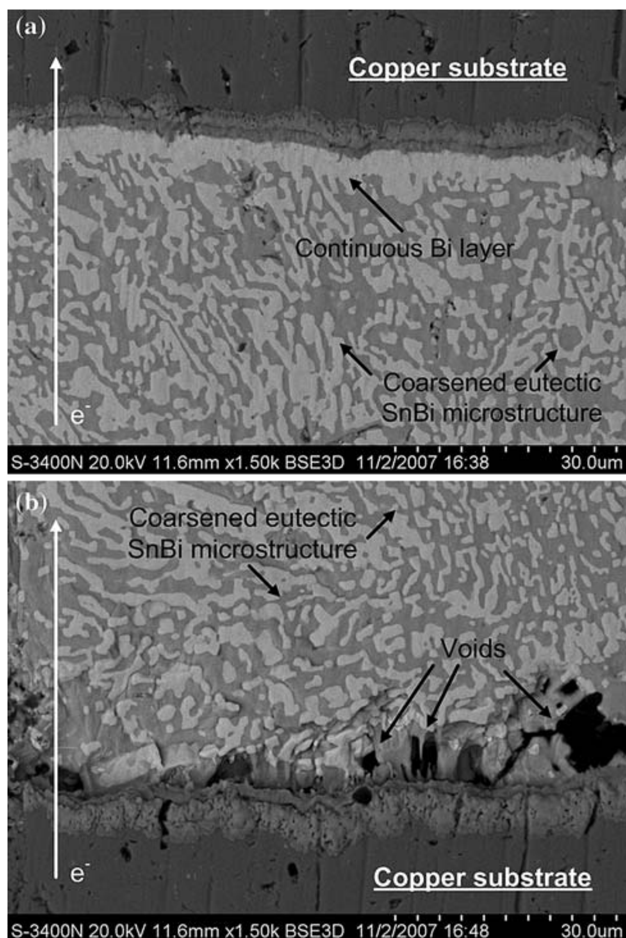

Fig. 7. Microstructural evolution of type I after 24 h of current stressing: (a) at the anode side; (b) at the cathode side.

in Sn-Pb solder by introducing an x-ray fluorescence spectroscopy technique. Their results indicated that initially both Sn and Pb migrated toward the anode as a consequence of EM. Our results showed the movement of both Sn and Bi atoms at the early stage of current stressing. Furthermore, it was also noted in the current study that the cross-sectioned surface of the specimen in type I, as shown in Fig. 8a, was no longer flat after current stressing. The accumulation of the Sn-rich phase near the cathode interface bulged, while the accumulation of the Bi-rich phase near the anode interface remained flat. This finding indicated that Bi tended to move ahead of Sn but without piling up due to its inherent brittleness. The generation of a compressive stress field due to the continuous movement of Bi could not trigger the obvious formation of hillocks at the anode interface which will be discussed in the following section. In addition, the migration of Sn appeared to be gradual from the cathode side toward the anode side, which caused the concentration of vacancies and eventually a valley near the cathode interface. Since the Sn-rich phase could not diffuse into the Bi-rich phase, and the Sn-rich phase was softer than the Bi-rich phase,

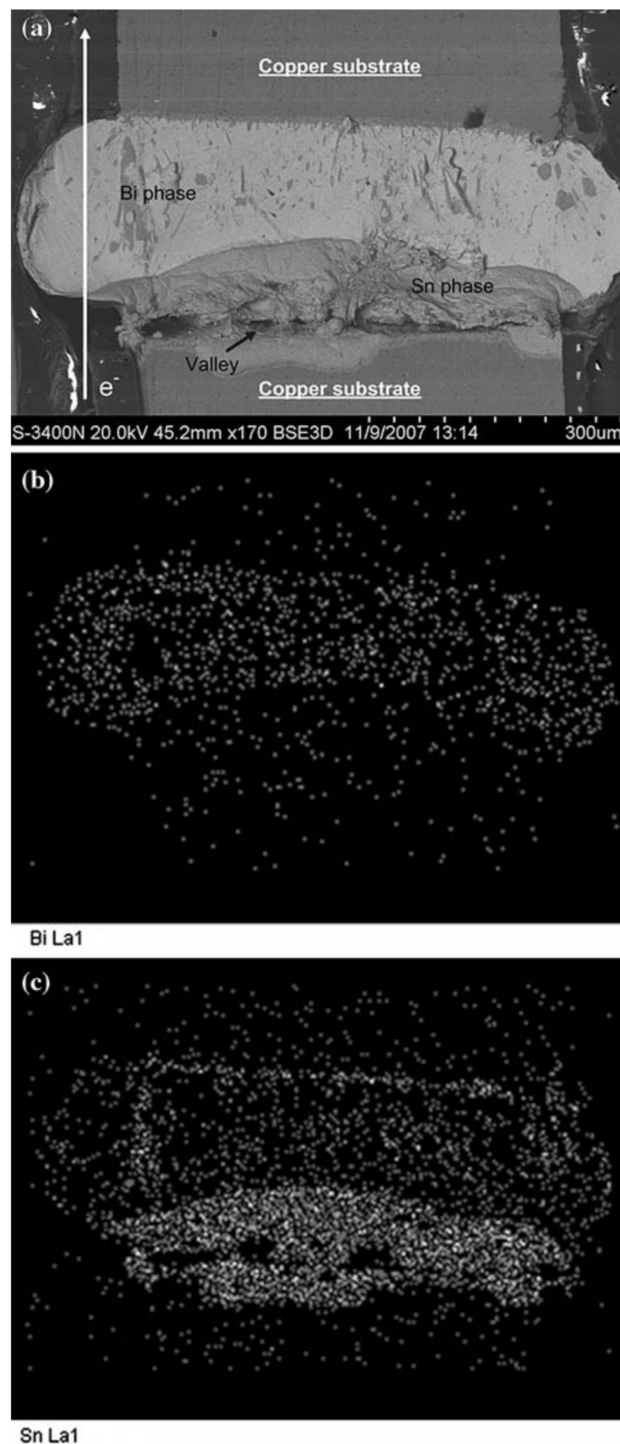

Fig. 8. Microstructural evolution of type I after 133 h of current stressing: (a) phase segregation of the Bi entity and Sn entity in the cross-section of type I; (b) elemental mapping of Bi at the anode side; (c) elemental mapping of Sn at the cathode side.

the surface of the Sn-rich phase eventually became fluctuated. As shown in Fig. 10, for the interface between the Sn-rich phase and Bi-rich phase, it is easy to find a height difference where the Sn-rich phase was higher than the Bi-rich phase, indicating that the Sn-rich phase was subjected to compressive

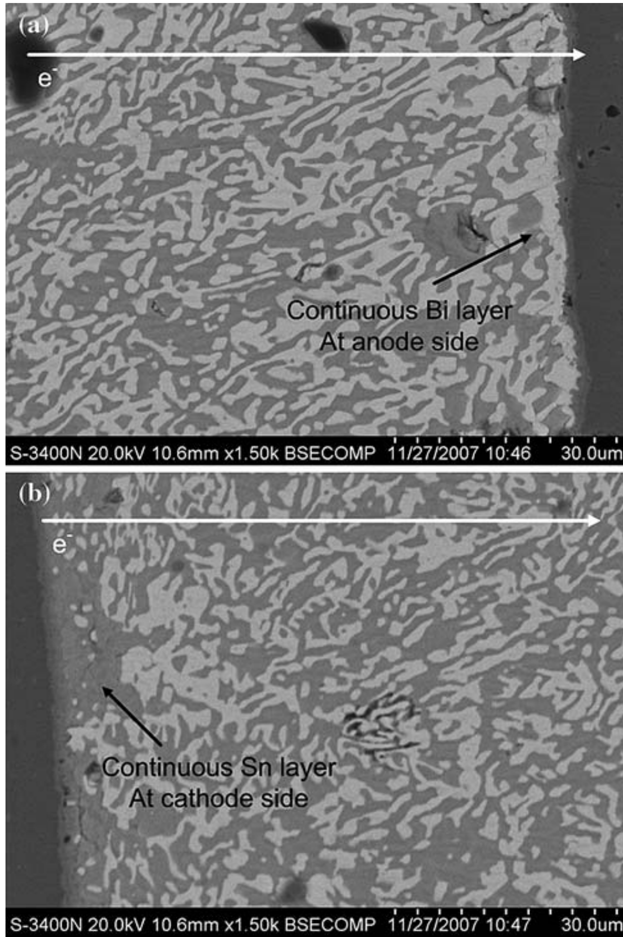

Fig. 9. Microstructural evolution of type III after 199 h of current stressing: (a) at the anode side; (b) at the cathode side.

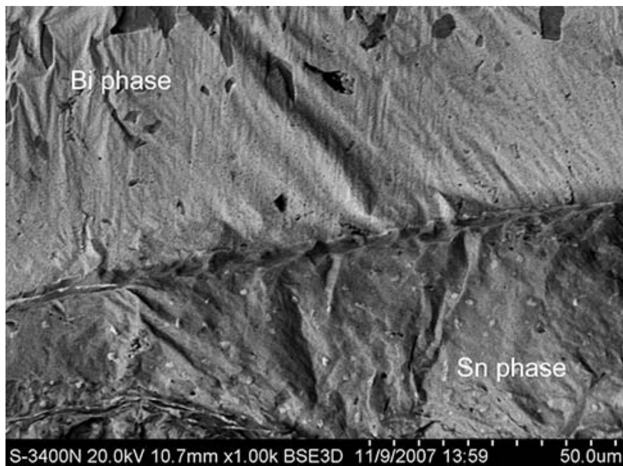

Fig. 10. Phase interface of the Sn- and Bi-rich phases in type I.

stress after the Bi-rich phase formed a barrier ahead of the Sn-rich phase. Figure 11 shows a schematic diagram of this process.

Within a metal interconnect, dislocations and grain boundaries are sources of vacancies, but the

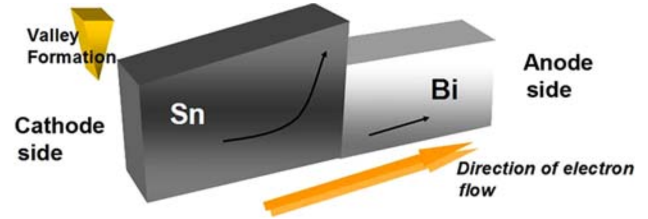

Fig. 11. Schematic diagram of metal/ions migration in eutectic Sn-Bi solder under high current density in type I.

free surface is generally the most important and effective source of vacancies, which means that the interface between the metal and its oxide is not a good source or sink of vacancies. When vacancies are removed without replenishment or added without an effective sink, the equilibrium vacancy concentration cannot be maintained, so a back stress will be generated.[17] However, there was no oxide formation in type III because of heat dissipation, which could cause the surface temperature to be lower than that in the interior region, thus the surface could act as a rigid wall or a protective layer to tie down the lattice in eutectic Sn-Bi and prevent it from moving. Thus, under the constraint of constant volume, the Sn atoms migrated in the reverse direction and accumulated at the cathode interface in type III.

Whisker/Hillock Growth at the Anode Side

Liu et al.[18] demonstrated that the growth of Sn whiskers can be accelerated by EM. In their study no obvious growth of Sn whiskers was observed after storage at room temperature. However, accelerated growth of Sn whiskers occurred when a high current density was applied. In types I, II, and III, no Sn whiskers were observed near the anode side during the EM test, because the dominant diffusion entities were Bi atoms. As illustrated in Fig. 12, the surface features of the Bi hillocks in type I exhibited rows of striations with a spacing of several microns. Such markings could be considered as an indication of materials being extruded as a consequence of compressive stresses from EM-induced mass flow towards the anode side. In type II, as illustrated in Fig. 13, there was a more serious solder extrusion region at the anode side after 24 h of current stressing, because type II was molten during the EM test. In liquid metals, the relative velocity, v, of an ion species due to an applied current field, E, can be written in terms of the effective valence, Z, and the friction coefficient, ξ:

$$v = \frac{Z|e|E}{\xi}, \quad (1)$$

where e is the electron charge. The direction of relative migration in a binary system is determined by the difference in the scattering cross-sections of the two species. The species with a

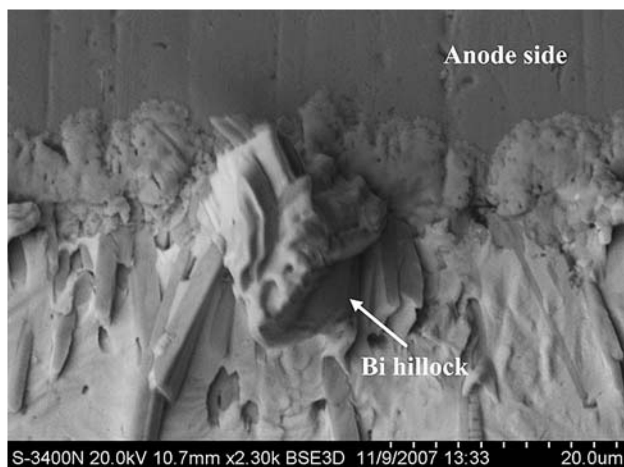

Fig. 12. Formation of Bi hillocks at the anode side after 133 h of current stressing in type I.

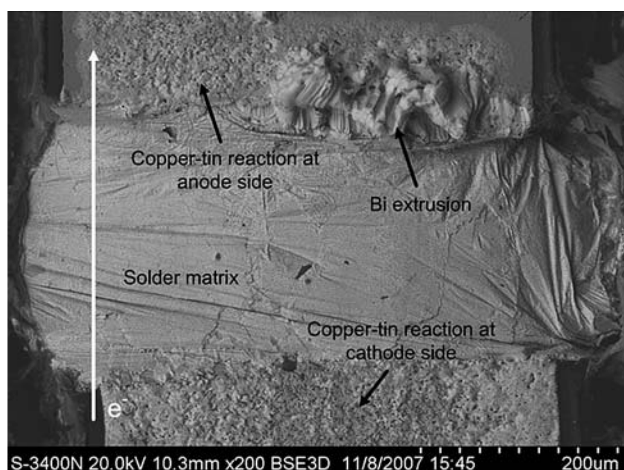

Fig. 13. Formation of Bi extrusion at the anode side after 24 h of current stressing in type II.

greater cross-section migrates to the anode, while the other species are displaced to the cathode. Since Bi has a greater scattering cross-section,[19] it should migrate to the anode side or act as a charged ion with a negative charge number, Z. Hillocks and whiskers were found at the anode side, as shown in Fig. 14a. In Fig. 14b, the oxide was cracked when the compressive stress was high enough and a whisker was extruded step by step. Figure 14c illustrates that the composition of the whisker was Bi. As shown in Fig. 15, in type III, the extra heat induced by Joule heating on the free surface of the specimen was dissipated by a fan, enabling the free surface to be fixed at room temperature. However, when the electrical current passed through the interior part of the solder reaction couples, Joule heating could obviously increase the interior temperature. As mentioned above, in type I, without heat dissipation, the Joule heating could increase the specimen temperature from 23°C to 50°C. Thus, in type III, the interior

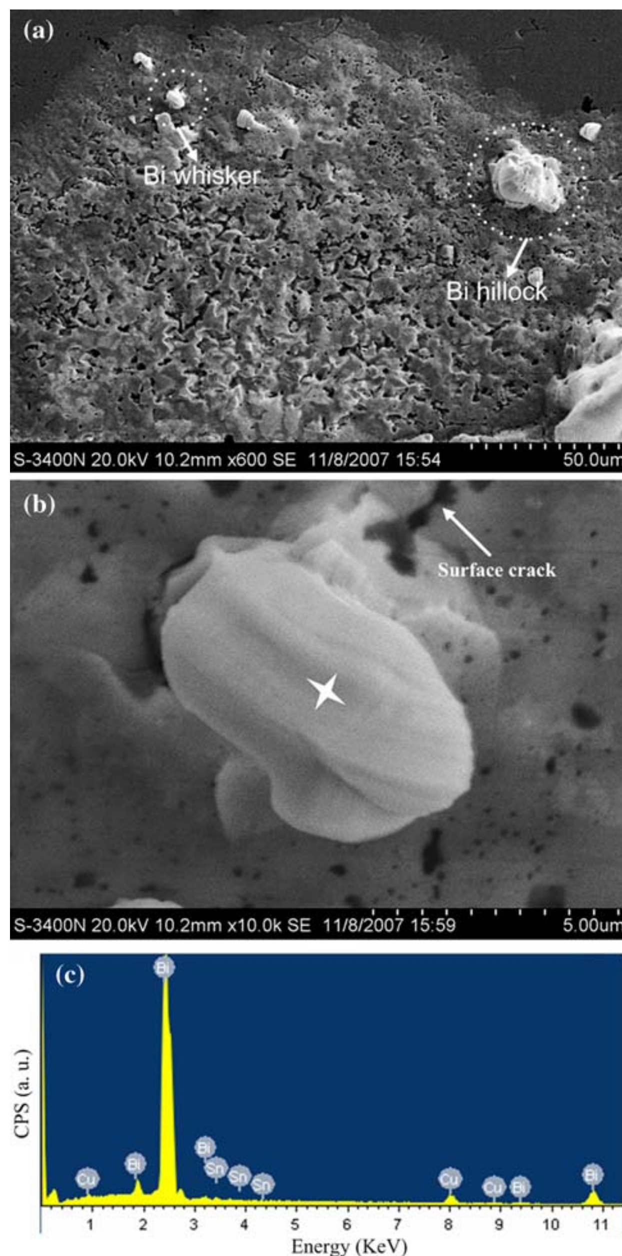

Fig. 14. Formation of Bi whiskers/hillocks at the anode side after 24 h of current stressing in type II: (a) region where the Bi whiskers/hillocks formed; (b) the Bi whisker; (c) EDX result of the Bi whisker.

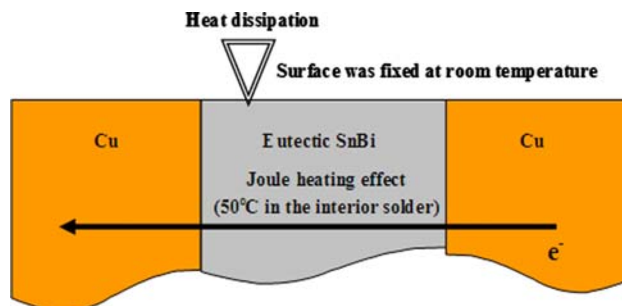

Fig. 15. Schematic of the diffusion mechanism in type III.

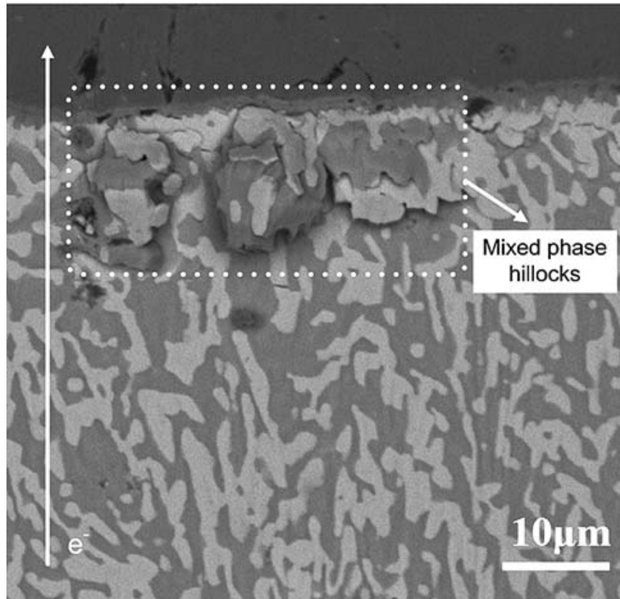

Fig. 16. Formation of the mixed phase of Sn/Bi hillocks at the anode side after 625 h of current stressing in type III.

temperature was 50°C while the free surface temperature was around 20°C. A higher temperature could prompt the mobility of metal atoms/ions; accordingly interior diffusion was faster than the surface diffusion. The accumulation of the Bi-rich phase at the interior anode side caused a mixed phase of Sn and Bi to pile up at the surface after 625 h of current stressing, as shown in Fig. 16.

CONCLUSIONS

The temperature dependence of the coarsening of the Bi-rich phase, the dominant diffusion entity, and hillock/whisker formation in eutectic Sn-Bi solder reaction couples under high current density (10^4 A/cm^2) were investigated. Three types of temperature conditions were employed in the test: pure Joule heating effect (50°C at the specimen surface), Joule heating effect plus thermal conduction (140°C at the specimen surface), and Joule heating dissipation (23°C at the specimen surface), respectively. After several to hundreds of hours of current stressing, three major conclusions were obtained:

1. Under appropriate Joule heating effect, the increased surface temperature reached about half the melting point of the eutectic Sn-Bi alloy, so the average size of the Bi-rich phase grew with increasing current stressing time. On the other side, the Bi-rich phase remained the same at the early stage of current stressing without any Joule heating effect. However, when the oven reinforced the Joule heating effect, the increased temperature could exceed the melting point of the eutectic Sn-Bi solder. The average size of the Bi-rich phase declined due to remelting and resolidification of the solder.
2. Bi accumulated at the anode side both at high (≥50°C) and low temperatures (≤23°C), whereas Sn exhibited the opposite direction of diffusion under the two temperature conditions. At high temperatures, the movement of Sn and Bi atoms was towards the anode side, but the Bi atoms formed a barrier ahead of the Sn atoms. The subsequently arriving Sn atoms were then subjected to a compressive stress and the surface of the Sn-rich phase fluctuated, leaving a valley near the cathode interface. At low temperatures, the flat surface of the eutectic Sn-Bi acted as a rigid wall or a protective layer to tie down the lattice and prevent the metal atoms/ions from moving. The generated back stress caused the Sn atoms to diffuse in the reverse direction towards the cathode side.
3. The growth of whiskers or hillocks can be accelerated by EM. The dominant diffusion entity was Bi in eutectic Sn-Bi solder alloy, thus Bi hillocks, Bi whiskers, and Bi extrusions were formed at the anode side under a uniform temperature distribution, indicating that surface diffusion was faster than interior diffusion. However, under a nonuniform temperature distribution, only a mixed phase bulged at the anode side, illustrating that interior diffusion was faster than surface diffusion.

ACKNOWLEDGEMENTS

The authors acknowledge financial support of this work from the the New Century Excellent Talent Support Program, Ministry of Education, and the Funding Project PHR (IHLB).

REFERENCES

1. H.B. Huntington and A.R. Grone, *J. Phys. Chem. Solids* 20, 76 (1961). doi:10.1016/0022-3697(61)90138-X.
2. I.A. Blech, *J. Appl. Phys.* 47, 1203 (1976). doi:10.1063/1.322842.
3. S.W. Chen, C.M. Chen, and W.C. Liu, *J. Electron. Mater.* 27, 1193 (1998). doi:10.1007/s11664-998-0068-5.
4. A. Lee, W. Liu, C.E. Ho, and K.N. Subramanian, *J. Appl. Phys.* 102, 053507 (2007). doi:10.1063/1.2777122.
5. S. Brandenburg and S. Yeh, *Proceedings of Surface Mount International Conference and Exhibition, SMI98* (San Jose, CA, Aug. 1998), p. 337.
6. T.Y. Lee, K.N. Tu, S.M. Kuo, and D.R. Frear, *J. Appl. Phys.* 89, 3189 (2001). doi:10.1063/1.1342023.
7. C.Y. Liu, C. Chen, C.N. Liao, and K.N. Tu, *Appl. Phys. Lett.* 75, 58 (1999). doi:10.1063/1.124276.
8. C. Chen and S.W. Liang, *J. Mater. Sci. Mater. Electron.* 18, 259 (2007). doi:10.1007/s10854-006-9020-8.
9. C.M. Chen and C.C. Huang, *J. Electron. Mater.* 36, 760 (2007). doi:10.1007/s11664-007-0150-4.
10. Q.L. Yang and J.K. Shang, *J. Electron. Mater.* 34, 1363 (2005). doi:10.1007/s11664-005-0191-5.
11. C.M. Chen and C.C. Huang, *J. Mater. Res.* 23, 1051 (2008). doi:10.1557/jmr.2008.0128.
12. L.T. Chen and C.M. Chen, *J. Mater. Res.* 21, 962 (2006). doi:10.1557/jmr.2006.0113.
13. C.E. Ho, A. Lee, and K.N. Subramanian, *J. Mater. Sci. Mater. Electron.* 18, 569 (2007). doi:10.1007/s10854-007-9263-z.
14. B. Tao, Y. Wu, H. Ding, and Y.L. Xiong, *Microelectron. Reliab.* 46, 864 (2006). doi:10.1016/j.microrel.2005.04.013.

15. J.G. Lee, F. Guo, K.N. Subramanian, and J.P. Lucas, *Solder. Surf. Mt. Technol.* 14, 11 (2002). doi:10.1108/09540910210427772.
16. C.E. Ho, A. Lee, K.N. Subramanian, and W. Liu, *Appl. Phys. Lett.* 91, 021906 (2007). doi:10.1063/1.2756292.
17. K.N. Tu, *Solder Joint Technology: Materials, Properties, and Reliability* (Springer, 2007).
18. S.H. Liu, C. Chen, P.C. Liu, and T. Chou, *J. Appl. Phys.* 95, 7742 (2004). doi:10.1063/1.1712019.
19. M. Shimoji, *Liquid Metals: An Introduction to the physics and Chemistry of Metals in the Liquid State* (London: Academic, 1977).